International Journal of Pure and Applied Mathematics
Volume 114 No. 12 2017, 289-297
ISSN: 1311-8080 (printed version); ISSN: 1314-3395 (on-line version)
url: http://www.ijpam.eu
Special Issue

ijpam.eu

Influence of Niobium on $Li_2Mn_4O_9$ for Lithium Ion Batteries

[1]K.K. Shaji, [2]S. Sharmila, [3]B. Janarthanan and [4]J. Chandrasekaran

[1]Department of Physics, Karpagam University,

Karpagam Academy of Higher Education, Coimbatore, India.

shajikk7@gmail.com

[2]Department of Physics, Karpagam University,

Karpagam Academy of Higher Education, Coimbatore, India.

sharmila.s@kahedu.edu.in

[3]Department of Physics, Karpagam University,

Karpagam Academy of Higher Education, Coimbatore, India.

janarthanan.b@kahedu.edu.in

[4]Department of Physics, Sri Ramakrishna Mission Vidhyala College of Arts and Science, Coimbatore, India.

jchandaravind@yahoo.com

Abstract

Highly oxidized $Li_2Mn_4O_9$ and Nbdoped $Li_2Mn_4O_9$ are synthesized using LiOH $2H_2O$ and MnO_2 and Nb_2O_5 as precursors. Effect of temperature, structural, morphological and electrical properties of both the materials are studied by SEM analysis particles are found to be in micron size and recognized by Electron Dispersive Spectroscopy. The chemical composition of Mn, O and Nb are spot out. 0.25 mole of Nb doped $Li_2Mn_4O_9$ unveil good electrical conductivity at 393 K. Hence Nb doped $Li_2Mn_4O_9$ is a viable cathode material for lithium ion- batteries.

Key Words: $Li_2Mn_4O_9$, solid state method, electrical conductance .

1. Introduction

Alternate energy sources have a great importance in now days. In future it will be forced to research and develop different alternate sources of energy in which the performance improved lithium ion batteries will have its own importance. Low cost, less environmental impact, high power makes $Li_2Mn_4O_9$ as a cathode material for rechargeable lithium ion cells [1]. Sony Energetic made first rechargeable lithium ion batteries in 1980 [2]. But lithium magnesium spinels reveal substantial capacity fading at elevated temperatures [3]

Though many reasons for the capacity fading have been suggested, one of the main reason is Mn dissolution. It is due to the presence of acid impurities at high electrode potentials lead to disproportionate reaction of Mn^{3+} to M_n^{2+} and M_n^{4+} [4]

T Inoue et al., [5] suggested that the increased lattice disorder in Li-Mn-O structure after the storage in the electrolyte at 55^0 is responsible for electrode capacity fading.Y. Matsuo etal .,[6] reported that the capacity fading also occurred due to the delithiation of the thin film $Li_2Mn_4O_9$ electrode in 1:1 EC: DMC +1 M L_i PF_6 electrolyte.

Thackeray et al., proposed that at the final phase of the discharge, the structural degradation of the spinel $Li_2Mn_4O_9$ occurred which pave way to the capacity fading of the spinel [7].

In the present study,$Li_2Mn_4O_9$is prepared using solid state method and substitute Nb in to the Mn sites of $Li_2Mn_4O_9$ in order to increase its conductivity and reduce the capacity fading of the material thereby look at the suitability of the material as cathode in lithium ion battery. Nb was selected as the dopant as it possess low resistivity, different oxidation state, low toxicity and used in various super conductors. The solid state method is preferred since it is simple, low cost and needs less time.

2. Experimental Method

Synthesis

The stoichiometric amount of LiOH H_2O and MnO_2 are blended together and pulverized well for 30 minutes. The homogeneous mixture thus obtained is heated in a muffle furnace at 700^0c for 6 hours. The resultant sample is finely grained and used for characterization. The same procedure has been adopted to prepare Niobium doped $Li_2Mn_4O_9$ sample with Nb_2O_5 as the starting precursor. The samples were named as $Li_2\,Mn_4O_9$ (L), $Li_2\,Mn_{3.75}\,Nb_{0.25}\,O_9$ (LN2) and $Li_2\,Mn_{3.5}\,Nb_{0.5}\,O_9$ (LN5).

Characterization

To recognize the structure of the materials the powder XRD(XPERT-3) with Cu Kα (λ=1.5 nm) was used in the range of $2\theta=10\text{-}80^0$ with a step size of 0.0130^0. The scanning electron microscopy is utilized to analyze the surface morphology of the material. By using EDAX the elemental compositions of the materials are confirmed. At a frequency range of 50 Hz to 50 KHz, the electrical conductivity is measured using H1OK1 3532 LCR H1TESTER.

XRD Analysis

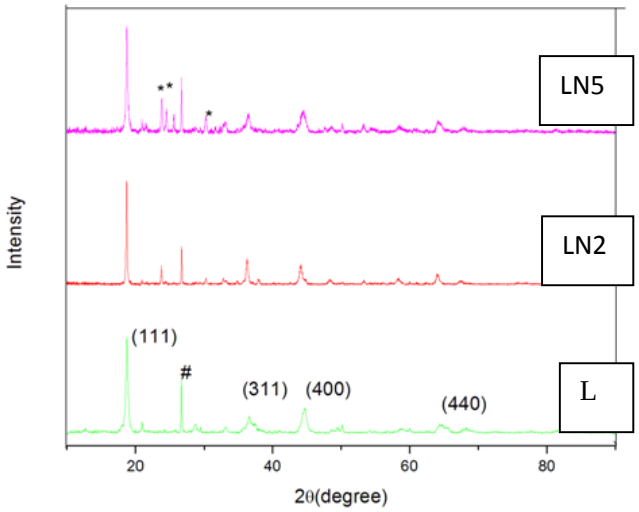

Figure 1: XRD spectrum of LP) $Li_2Mn_2O_9$ LN2) $Li_2Mn_{3.75}Nb_{0.25}O_9$ LM5) $Li_2Mn_{3.5}Nb_{0.5}O_9$

Table 1: XRD parameters

Material	Lattice constant(Å)	Cell Volume $(Å)^3$	Lattice density $(g\ cm^{-3})$	Grain size (nm)
$Li_2Mn_4O_9$	8.164	544.217	23.923	41
$Li_2Mn_{3.75}Nb_{0.25}O_9$	8.2133	554.055	23.453	50.4
$Li_2Mn_{3.5}\ Nb_{0.25}O_9$	8.1804	547.44	22.916	33.6

The XRD patterns of pristine and Nb doped $Li_2Mn_4O_9$ are shown in the figure 1. Since the sharp and well defined peaks obtained shows the highly crystalline nature of the material. The obtained peaks are in compatible with JCPDS card no (88-1608) indicating the formation of cubic spinel structure. Some impurity Peaks are detected at figure 1A at 26.6^0 in the parent sample and is identified as SiO_2 which is unveiled in the EDAX analysis also. This is due to the fewer amount of impurities present in the source. Similarly in the fig 1B and 1C additional peaks have been observed at 23^0, 31^0 indicates the presence of $LiNbO_3$JCPDS (74-2237). The lattice constant, lattice density, cell volume and grain size of the pristine and doped material are calculated and found to be

compatible with JCPDS card value. Since the ionic radius of Nb(78nm) is high compared to Mn(72 pm) the lattice is found to be increasing with the increase in concentration as per Vegard's law. [8]. Since the cell volume increases, the lattice density is found to be decreased. The grain size of $Li_2Mn_{3.75}Nb_{0.25}O_9$ is highin par with pristine $Li_2Mn_4O_9$ due to the lattice expansion of the material and for 0.5 mole it found to be decreased. [9].

Morphological Analysis

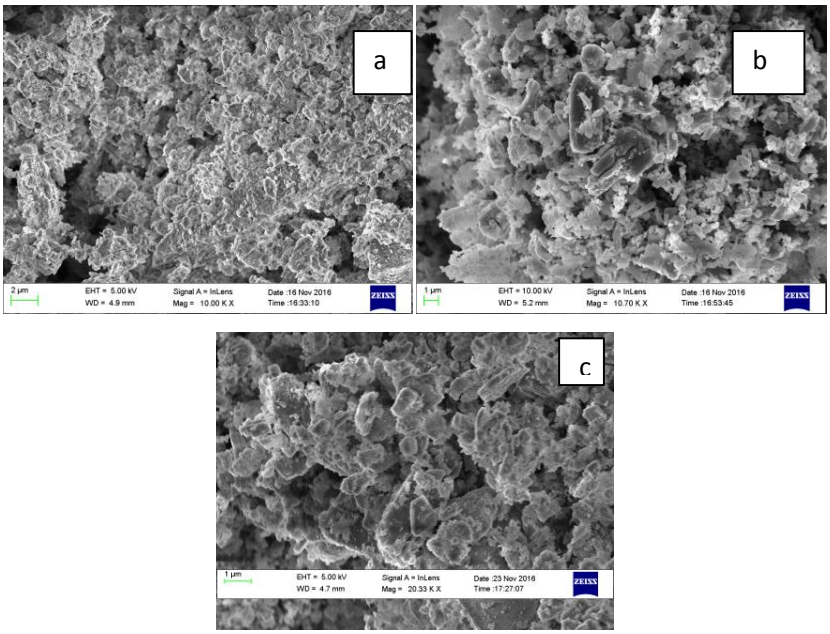

Figure 2: SEM images of a) L b) LN2 c) LN5

The SEM images of pristine and doped materials are depicted in the figure 2. It is clear from the SEM images that the particles are uniformly distributed and the size of the particles are measured in micrometer length which is in good agreement with the results obtained from researches.

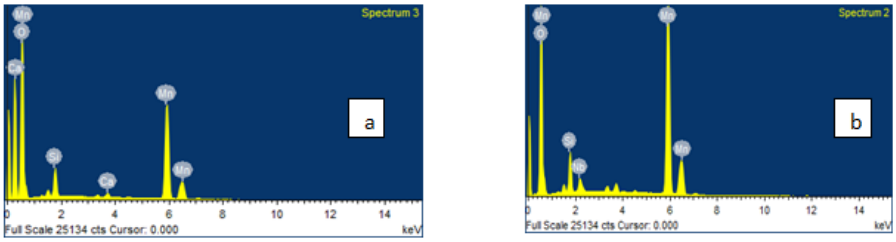

Figure 3: EDAX spectrum of a) L b) LN2

The chemical composition of the materials is identified using EDAX. Figure 3 [a-b] depicts the EDAX analysis of the material. Analyzing the figure, we can find the presence of Mn, O and Nb is found.

Electrical Properties

The electrical properties of the materials have been investigated over a wide range of frequency and temperature using the impedance spectroscopy. Figures 4(a-c) exhibits Nyquist plot(cole-cole plot) of pristine,doped samples at low temperature from 60^0C to 120^0C. The formation of the semicircular region at all temperatures from 60^0-120^0 C. The formation of the semi circular region at all temperatures elucidates the absence of grain boundary effect. The conduction happens only through the bulk of the material [10]. The interception of semi circle on the X- axis gives the bulk resistance and is found to be decreased with increase in the temperature. This shows the negative temperature coefficient of resistance (NTCR property). Hence the material is a semiconductor.

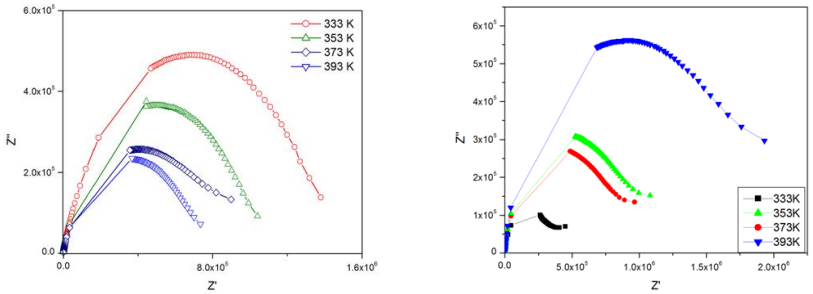

(a) (b)

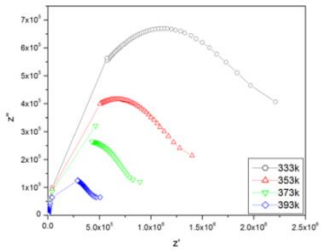

(c)

Figure 4: Cole-Cole plot of a) L b) LN2 c) LN5

By using the relation, $2\pi\gamma_{max}R_bC_b=1$,the bulk capacitance can be enumerated. The capacitance obtained in the order of pico Farad. By using the relation $\sigma = \frac{\ell}{R_{bA}}$ Scm^{-1}, the ionic conductivity of the materials are calculated where R_b is the bulk resistance, *l*the thickness and A is the area of the pelletized sample. The values are given in the table 2.It is found that as the temperature increases due to thermally activated mobile charge carriers, the conductivity also increases [11]. The electrical conductance of $Li_2Mn_4O_9$, Li_2 $Mn_{3.75}Nb_{0.25}O_9$and Li_2 $Mn_{3.5}Nb_{0.5}O_9$ is shown in the figure 5 (a-c). The curve explicit in two regions.

a) Low frequency regions which are the frequency independent plateau and

b) High frequency dispersive region [12].
c) The low frequency region corresponds to σ dc conductivity and high frequency region reveals the ac conductivity of the materials. With the increase of temperature, the conductivity also increases as per Jonscher's universal power law $\sigma(\omega) = \sigma dc + A\omega$[13]

The charge carrier concentration, hopping frequency and mobility of the material is calculated using the non linear curve fitting. For all samples, the conductivity is increasing with the increasing temperature. 0.2 moleNb doped $Li_2Mn_4O_9$ at 393 Kelvin shown a high conductivity of $31x10^{-7}$ S $cm^{-1.}$

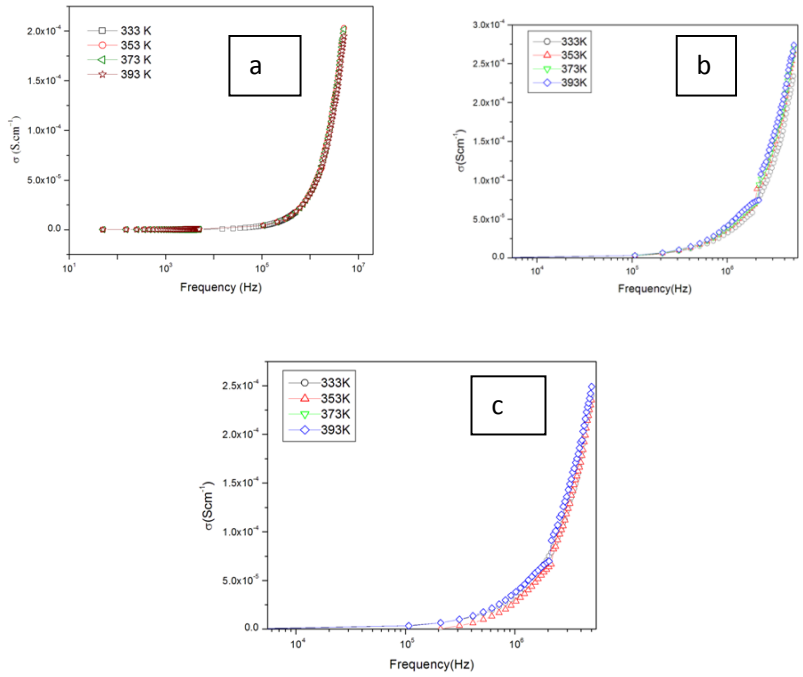

Figure5: Conductance Spectrum of a) L b) LN2 c) LN5

Table 2: Electrical Parameters

Material	Temp. (K)	R_b x 10^5	C_b (pF)	σ_{dc} (10^{-7})	ωp x 10^4 (Hz)	N x 10^{-9} (S cm^{-1} kHz^{-1})	μ × 10^{20} ($cm^2V^{-1}s^{-1}$)
L	333	13.80	38.7	1.05	0.30547	10.758	0.6099
	353	10.30	30.9	2.56	0.31970	26.666	0.6000
	373	8.940	3.56	2.856	0.9273	10.841	1.6190
	393	7.320	5.19	3.608	0.6798	19.799	1.1391
LN2	333	19.28	27.7	14.6	111.79	1.72	210
	353	10.83	29.4	21.6	275.91	1.03	489
	373	9.704	32.8	22.6	371.04	4.8	622
	393	3.868	82.3	31	963.04	6.19	1530
LN5	333	22.138	46	12	70.00	1.72	131
	353	14.102	37.9	13	102.9	1.03	182
	373	8.407	37.9	13.5	758.16	4.8	127
	393	4.658	68.4	14.5	316.81	6.19	504

3. Conclusion

Defect spinel $Li_2Mn_4O_9$ and Nb doped $Li_2Mn_4O_9$ were successfully synthesized using solid state method at 700^0C in two different concentrations. The structural and morphological parameters of the materials are confirmed using XRD, SEM and EDAX analysis. With the increase in temperature, the bulk resistance of the sample decreases and the least value has obtained for $Li_2\ Mn_{3.75}Nb_{0.25}O_9$ at 393 K and it shows a high conductivity of $31x10^{-7}$ S cm^{-1}. Hence it is concluded that $Li2Mn_{3.75}Nb_{0.25}O_9$ may serve as a good cathode material for lithium ion batteries.

References

[1] Guyomard D., Tarascon J.M, The carbon/Li1+ xMn2O4 system. Solid State Ionics 69(3-4) (1994), 222-237.

[2] Mizushima K., Jones P.C., Wiseman P.J., Good enough J.B, LixCoO2 (0< x<-1): A new cathode material for batteries of high energy density, Materials Research Bulletin 15(6) (1980), 783-789.

[3] Arora P., White R.E., Doyle M, Capacity fade mechanisms and side reactions in lithium-ion batteries, Journal of the Electrochemical Society 145(10) (1998), 3647-3667.

[4] Jang D.H., Shin J., Oh S.M, Journal of Electrochemical Society, 143(1996), 2204.

[5] Inoue T., Sano M., An investigation of capacity fading of manganese spinels stored at elevated temperature, Journal of The Electrochemical Society 145(11) (1998), 3704-3707.

[6] Matsuo Y., Kostecki R., McLarnon F., Surface Layer Formation on Thin-Film $LiMn_2O_4$ Electrodes at Elevated Temperatures, Journal of The Electrochemical Society 148(7) (2001), A687-A692.

[7] Thackeray M.M., Shao-Horn Y., Kahaian A.J., Kepler K.D., Skinner E., Vaughey J.T., Hackney S.A, Electrochem. solidstate Lett. 1(7) (1998).

[8] Nithya V.D., Sharmila S., Vediappan K., Lee, C.W., Vasylechko L., Selvan R.K, Electrical and electrochemical properties of molten-salt-synthesized 0.05 mol Zr-and Si-doped $Li_4Ti_5O_{12}$ microcrystals, Journal of Applied Electrochemistry 44(5) (2014), 647-654.

[9] Yan-Jing., Hoa-Ling Wang-Qiong-yu Lai, Journal of Solid State Chemistry 15 (2011).

[10] Shenouda A.Y., Murali K.R, Electrochemical properties of doped lithium titanate compounds and their performance in lithium rechargeable batteries, Journal of Power Sources 176(1) (2008),

332-339.

[11] Selvan R.K., Augustin C.O., Šepelák V., Berchmans L.J., Sanjeeviraja C., Gedanken A, Synthesis and characterization of $CuFe_2O_4/CeO_2$ nanocomposites, Materials Chemistry and Physics 112 (2) (2008), 373-380.

[12] Bhaskaran, Vanadium SenthilKumar, Ramakrishna Kalaisevan, Palanisamy Vinothbabu, Mater.Chem.Phy. 130 (1-2) (2011), 285-292.

[13] Jonscher A.K, The universal' dielectric response, nature 267 (1977), 673-679.